Journal of Textile Science and Technology, 2022, 8, 89-106
https://www.scirp.org/journal/jtst
ISSN Online: 2379-1551
ISSN Print: 2379-1543

Dyeing Thermodynamics and Supramolecular Structure of Lac Red on Protein Fibers

Kewen Fu[1,2], Jian Li[1,2], Dongkai Qin[1,2], Luwei Shi[1,2], Xiangyu Ni[1,2], Kaikai Zhao[1,2], Dequan Xu[2,3*], Ailin Yuan[1,2], Chunling Zheng[1,2*]

[1]College of Food Science and Light Industry, Nanjing Tech University, Nanjing, China
[2]Institute of Textile Auxiliary and Ecological Dyeing Finishing, Nanjing Tech University, Nanjing, China
[3]College of Chemistry and Chemical Engineering, Wuhan Textile University, Wuhan, China
Email: *zhengchunling@njtech.edu.cn

How to cite this paper: Fu, K.W., Li, J., Qin, D.K., Shi, L.W., Ni, X.Y., Zhao, K.K., Xu, D.Q., Yuan, A.L. and Zheng, C.L (2022) Dyeing Thermodynamics and Supramolecular Structure of Lac Red on Protein Fibers. *Journal of Textile Science and Technology*, **8**, 89-106.
https://doi.org/10.4236/jtst.2022.82008

Received: April 15, 2022
Accepted: May 23, 2022
Published: May 26, 2022

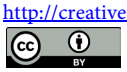

Abstract

The dyeing temperature of natural dye lac red on two kinds of natural protein fibers was studied, and the interaction between dyestuff and fiber was discussed through thermodynamic study and density functional theory (DFT) calculation. The optimum temperature for lac red dyed silk was 60˚C and wool showed a better response at 90˚C. The thermodynamics study revealed good Nernst isotherm and Freundlich adsorption models respectively, and the lac dye adsorption processes were both spontaneous and exothermic. The potential interaction of Laccaic acid A with the external environment by electrostatic potential and atomic charge distribution was first explored. With molecular simulation, Laccaic acid A and glycine composed 8 stable complexes. Then, typical hydrogen bonds, bond length, and binding energy, *etc.* were analyzed. The results revealed lac red on silk and wool fabric mainly depended on the weak hydrogen bonds and van der Waals force which determined the low dye fastness.

Keywords

Natural Dye, Lac Red, Wool, Silk, Dyeing Thermodynamics, DFT Calculation, Wavefunction

1. Introduction

As the upscale textile fibers in the textile industry, wool and silk exhibit the inherent excellent characteristics of soft luster, luxurious hand, strong moisture absorption, preferable heat insulating ability, better anti-wrinkling performance and stain-resistance ability, especially comfortable to wear. Wool fibers and silk

fibers consist of protein in which the repeated unit is an amino acid. The amino acids are linked together by peptide bond (-CO-NH-) to form a protein structure. The most important component in wool is keratin that is amphoteric and a complex protein comprised of diversified α-amino acid residue [1] [2]. The key component in silk is fibroin protein which is mainly composed of glycine, accounting for about 70%. Natural dyes are believed to be suitable for the coloration of wool and silk fabrics, because of their generally low toxicity, reduced pollution and biodegradable nature [3].

Lac dye is a unique dye material of animals extracted from stick lac which is a secretion of the insect *Coccus lacca* (Laccifer lacca Kerr). The insect *C. lacca* is often found in South and Southeast Asia, especially in Thailand and India [4]. Lac dye is composed of a series of water-soluble anthraquinone molecules, of which laccaic acids A and B are present in major quantities, whereas laccaic acids C, D and E are minor components [5] [6] [7] (**Figure 1**). The use of lac dye in the dyeing of silk and leather seems to have been known to the Chinese some 4000 years ago.

Textile is our primary goods and the question of whether the manufacturing processes and materials for textile meet our health requirements has aroused wide attention. Conventional wisdom leads to the belief that natural dyes are friendlier to the environment than their synthetic counterparts. Lac dye is used extensively as a natural food additive [8], and in cosmetics [8] [9], as well as a colorant for silk and cotton dyeing [4], but the fastness properties and reproducibility to give consistency in production are still problems to be solved. As part of the approach to tackle these problems, the study of thermodynamics in the dyeing process and supramolecular structure simulation are crucial for understanding the behavior of lac red in the actual environment and facilitating its application in practice.

2. Experiments

2.1. Materials and Instrumentations

Wool and silk were obtained from textile market. Lac dye is purchased from Dongyang Shennong Textile Technology Co., Ltd, Zhejiang, China. All other

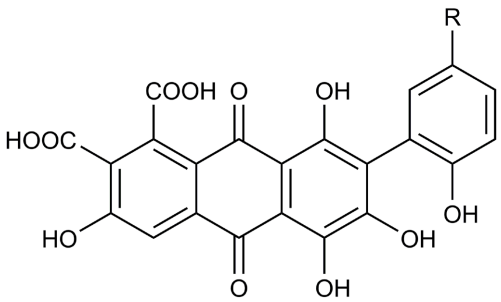

Laccaic acid A	R=$CH_2CH_2NHCOCH_3$	MW 537
Laccaic acid B	R=CH_2CH_2OH	MW 496

Figure 1. The molecular structure of Laccaic acids A and B.

chemicals and reagents used were of analytical grade *i.e.*, glacial acetic acid and Sodium acetate anhydrous were bought from Sinopharm. The apparatuses, thermostatic water bath (HH-4), datacolor (600), vacuum pump (SHB-III) and UV/Visible spectrophotometer (Cary60) were used. The software, Guassian 16 program, Multiwfn 3.8 code and VMD 1.9.4 program were used for calculation.

2.2. Dyeing Process Optimization

The dyeing process influenced under variable temperature since temperature affects physicochemical properties. The dyeing was carried out using 6% o.w.f. of lac dye, at a material to liquor ratio of 1:60 and maintaining at a pH value of 3.6 for 60 min. Different temperature (50˚C, 60˚C, 70˚C, 80˚C, 90˚C and 100˚C) for the optimization of the dyeing parameters were studied.

The *K/S* values were evaluated at D_{65} light source and 10˚ perspective using Datacolor600. Each fabric to be tested was folded in 4 layers, and the color characteristic values of 4 different parts were measured and the average value was taken.

2.3. Dyeing Thermodynamics Experiments

First, the fabric was dried in drying oven. Then, we weighed 12 samples of dried fabric and each sample was 0.5000 g. Subsequently, these silk samples were carried out in dyebaths that the bath ratio was 1:60 and the pH was 3.6 severally at 50˚C, 60˚C for 60 min, and the wool samples were dyed at 90˚C and 100˚C respectively. Each dyeing was done for different dye shades of 3, 4.5, 6, 7.5, 9, 10.5, 12, 13.5, 15, 16.5, 18 and 19.5 percent o.w.f. The dyed samples were respectively rinsed with 75mL water in order to remove non-absorbed dyes and rinse water was mixed with homologous dyeing residue. We respectively measured the absorbance of each mixed dyeing residue and drew the adsorption isotherms, and dyeing affinity, dyeing enthalpy and dyeing entropy were also calculated using statistical functions [10] [11].

2.4. Supramolecular Structure Simulation Experiments

The conjecture was that there was obvious hydrogen bonding interaction between lac red and silk fiber because of abundant hydroxyl groups and carboxyl groups in silk fiber molecule and lac red [12]. Here Laccaic acid A and glycine holding a large where be chosen as research object to analyze and discuss the significance of combination manners and space structures when lac red was used for dyeing silk fabric.

Density functional theory (DFT) calculations were used to optimize the configuration of Laccaic acid A and glycine using Gaussian 16 program (Version G16 B.01, Gaussian Inc. Wallingford CT, 2016) [13]. The geometries of Laccaic acid A-glycine complexes were also optimized using Gaussian 16 program. All geometry optimizations were carried out with B3LYP/6-31G(d) basis set at 60˚C under 1 atm pressure [14] [15] [16].

Glycine molecule was positioned near polar groups of Laccaic acid A molecule. Then the minimum energy of different Laccaic acid A-glycine complexes (also with the absence of imaginary frequencies) was chosen as the optimum geometry. The optimized structural parameters were used for the analysis of hydrogen bonds, dipole moment and binding energy of the complexes.

Electrostatic potential (ESP) and non-covalent interaction (NCI) map on the basis of the geometry and wavefunction at B3LYP/6-31G(d) level were performed with the Multiwfn 3.8 code [17]. All isosurface maps were rendered by VMD 1.9.4 program [18] based on the outputs of Multiwfn. Unless otherwise specified, the default settings are used throughout our calculations. Followed by Bader *et al.* [19], the vdW surface referred throughout this paper denotes the isosurface of $\rho = 0.001$ e/bohr^3.

3. Results and Discussion

3.1. Effect of Temperature

The results of the studies on the influence of temperature on the dyeing effect of lac dye onto silk and wool are shown in **Figure 2**. Results show that: it is clear that the *K/S* values increases first and then decreases with increase in dyeing temperature in both the dyeing of silk and wool. The value of *K/S* reflects the apparent color depth of the fabric. The higher the value of *K/S* is, the darker the color of the fabric is, indicating that the dyeing fabrics obtained better dyeing effect. The optimum temperature for silk was 60˚C and wool showed better response at 90˚C. The low color strength on wool at lower temperature was due to the tight structure of epicuticle layer existing on wool surface which had great resistance to the diffusion of dye.

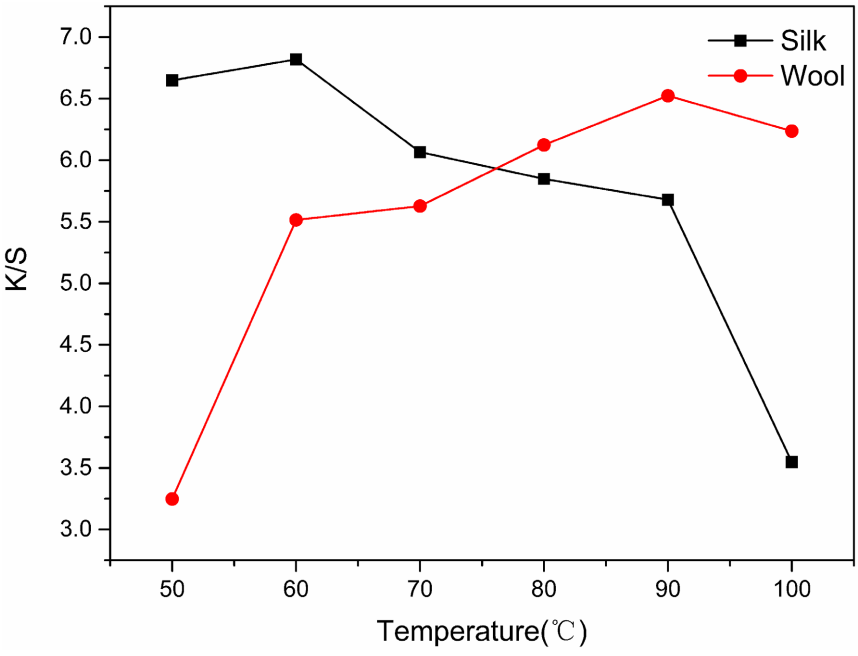

Figure 2. Effect of dyeing temperature on color strength of silk and wool.

3.2. Dyeing Thermodynamics Research of Lac Dye on Silk and Wool Fabric

3.2.1. Adsorption Isotherms

In order to further explore the adsorption isotherms of lac red on wool and silk fiber, two parameter equations including Nernst and Freundlich equation were used to analyze the experiment data.

The Nernst [20] Equation (1) is an important model for the analyzing of the adsorption process of dyes:

$$C_f = K_N C_s \tag{1}$$

where C_f (mg/g) and C_s (g/L) are the adsorption amount of dyes on fiber and the concentrations of dyes in final solutions, respectively; K_N is the distribution coefficient. The line could be obtained through the plotting C_f against C_s (**Figure 3** & **Figure 4**). The index (R^2) was used to evaluate the fitness of experiment data and thermodynamic models.

In addition, the Freundlich [21] [22] Equation (2) is another important model about the adsorption process of dyes.

$$\lg C_f = \lg K_F + n \lg C_s \tag{2}$$

where K_F and n are the adsorption constant and the adsorption intensity, respectively. The line of ln C_f versus ln C_s is shown in **Figure 5** & **Figure 6**.

It is worthy noticing that the correlation coefficients R^2 are in the range of 0.9337 to 0.9859 obtained by linear fitting, indicating the adsorption process of lac red on silk and wool fiber showed better agreement with the Nernst model and the Freundlich model. The fixation and the adsorption of the dye molecules at the surface or the interior of the fiber are governed by affinity between natural dyestuff of lac red and protein fiber. So, the inference natural dyestuff of lac red

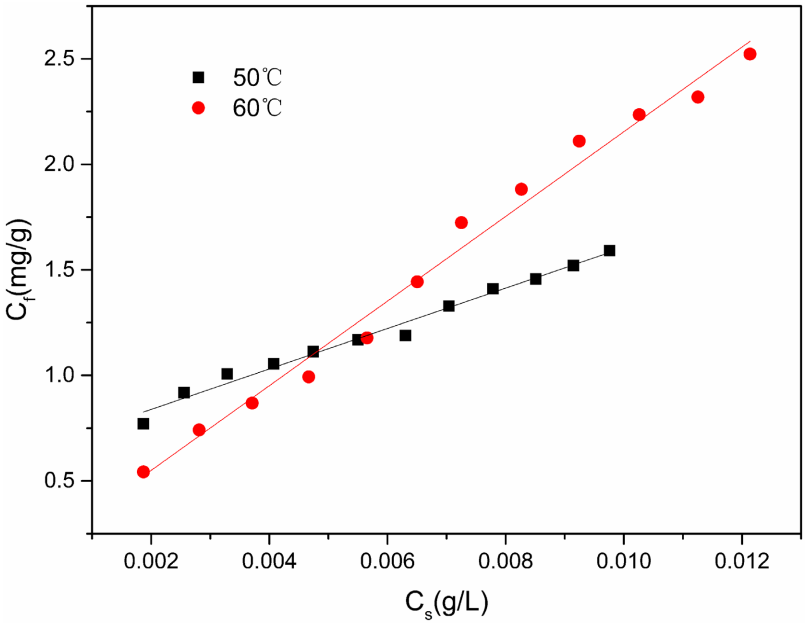

Figure 3. The Nernst model of lac red on silk fiber.

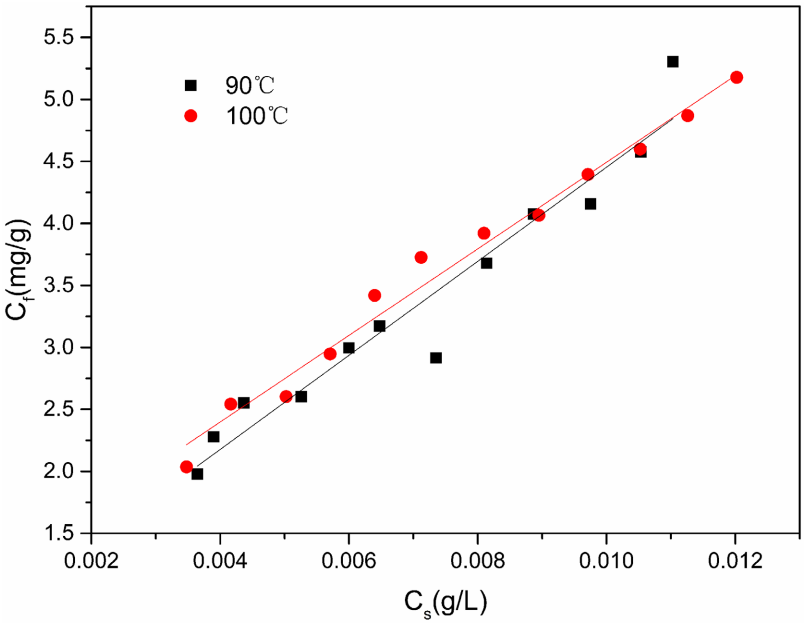

Figure 4. The Nernst model of lac red on wool fiber.

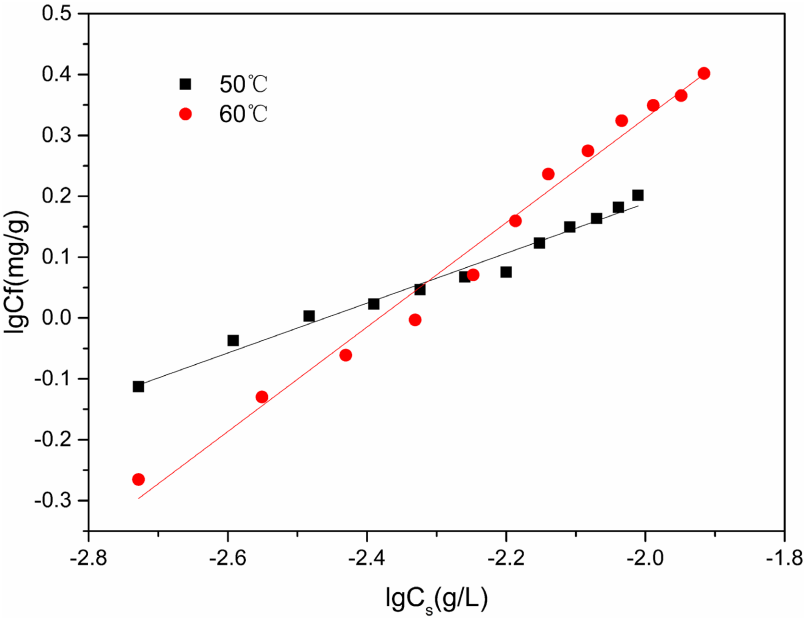

Figure 5. The Freundlich model of lac red on wool fiber.

dyes silk and wool fiber probably mainly by van der Waals force and hydrogen bonds.

3.2.2. Calculation of Standard Affinity, Dyeing Enthalpy and Dyeing Entropy

The adsorption property of luteolin on wool fiber is similar to the adsorption of disperse dyes on polyester fiber and the nature of luteolin adsorption pertains to distribution mechanism [23]. The thermodynamic parameters such as standard affinity ($-\Delta\mu^{\theta}$), dyeing enthalpy (ΔH) and dyeing entropy (ΔS) were computed

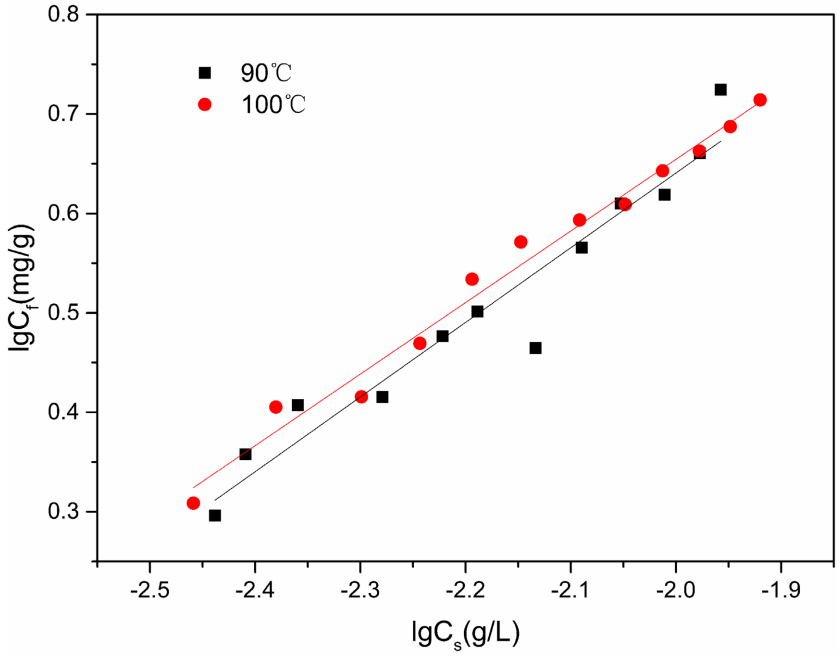

Figure 6. The Freundlich model of lac red on wool fiber.

Table 1. Thermodynamic parameters for lac red on silk and wool fiber.

	Temperature/˚C	Standard affinity $-\Delta\mu$/(kJ·oml^{-1})	Standard affinity ΔH/(kJ·mol^{-1})	Standard affinity ΔS/Kj (mol·K^{-1})
silk	50	8.48	−2.34	0.019
	60	8.67		0.019
wool	90	12.11	−26.28	−0.039
	100	11.73		−0.039

as shown in Equations (3)-(5) [11] [24].

$$-\Delta\mu^0 = RT\ln\left[D_f\right]/\left[D_s\right] \tag{3}$$

$$\Delta H = \left(T_2\Delta\mu_1 - T_1\Delta\mu_2\right)/\left(T_2 - T_1\right) \tag{4}$$

$$-\Delta\mu^0 = T\Delta S - \Delta H \tag{5}$$

where, D_f and D_s are the concentration of dye on the fiber and in the dyebath respectively, T is the temperature and R is a constant standing for 8.314 J·(mol·K)$^{-1}$. The thermodynamic parameters obtained at different temperatures are presented in Table 1.

Table 1 shows the negative values of $\Delta\mu$ and ΔH that lac dye adsorption is a spontaneous and an exothermic process. Within certain temperature range, the affinity of lac red on silk fiber increased in the wake of the increase of temperature, and the affinity of lac red on wool fiber decreased with the increase of temperature. The affinity indicates the trend of the sorption behavior of dyes onto fibers and the higher value reflects more energetically favorable sorption [25], which is consistent with the previous conclusion that the optimal dyeing tem-

peratures for silk and wool are 60˚C and 90˚C, respectively. The ΔS represents the degree of randomness of dye molecule and the negative value of the ΔS manifests the decreased randomness after the adsorption of lac dye on wool [26].

3.3. Supramolecular Structure of Lac Red on Silk Fabric

3.3.1. Electrostatic Potential and Atomic Charge Distribution of Laccaic Acid A

Geometries of Laccaic acid A and glycine optimized with B3LYP/6-31G(d) basis set were shown in **Figure 7**.

ESP on molecular surface is critical for understanding and predicting intermolecular interaction [27] [28] [29] [30] [31]. In-depth investigation of ESP of Laccaic acid A must be very helpful for deeper understanding of the important interaction between Laccaic acid A and glycine molecular. The ESP mapped vdW surface of Laccaic acid A is shown in **Figure 8(A)**. The surface area in each ESP range is plotted as **Figure 8(B)**. The two sections of Fig. 8 show that most part of vdW surface of Laccaic acid A have positive value of ESP and low ESP value (*i.e.* within −10 to +10 kcal/mol), but there is also a large portion vdW surface has large negative value of ESP (*i.e.* <−30 kcal/mol); they attribute to the surface close to the carbonyl group and the oxygens of the carboxyl group and hydroxyl group which have the obvious negative charge. Only tiny part of the vdW surface has ESP value larger than +40 kcal/mol, and they stem from the hydrogens in hydroxy and carboxyl group. The global minima and maxima of ESP on the surface are −48.14 and +69.89 kcal/mol, and correspond to the oxygen in carbonyl group and the hydrogen in carboxyl group, respectively. It has lower negative extrema at the 9-quinone carbonyl oxygen group compared with the potential at the other quinone group because of the delocalization of the lone pairs of electrons from the phenolic groups at positions 3 and 6 [32].

The charge of each atom was obtained by Mulliken charge analysis method. Atomic charge distribution of Laccaic acid A was −0.682e to 0.572e, C53 in amide group showed highest positive charge of +0.572e. O17, O18, O21 and O22 in carboxyl group, O32 and O33 in quinone group and O24, O26, O28, O30 and O42 in hydroxyl group showed negative charges of O17 (−0.458), O18 (−0.554), O21 (−0.437), O22 (−0. 559), O32 (−0.477), O33 (−0.464), O24 (−0.620), O26

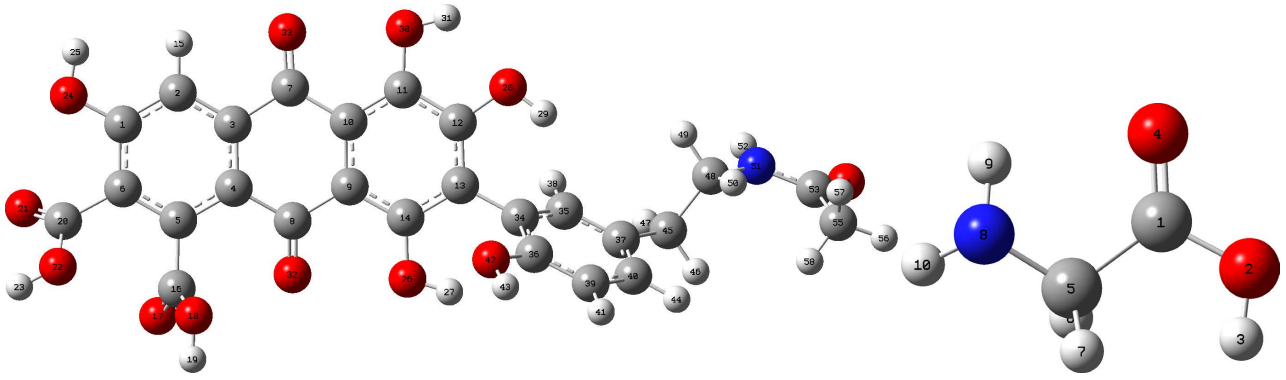

Figure 7. Geometries of Laccaic acid A and glycine optimized with B3LYP/6-31G(d,p) basis set.

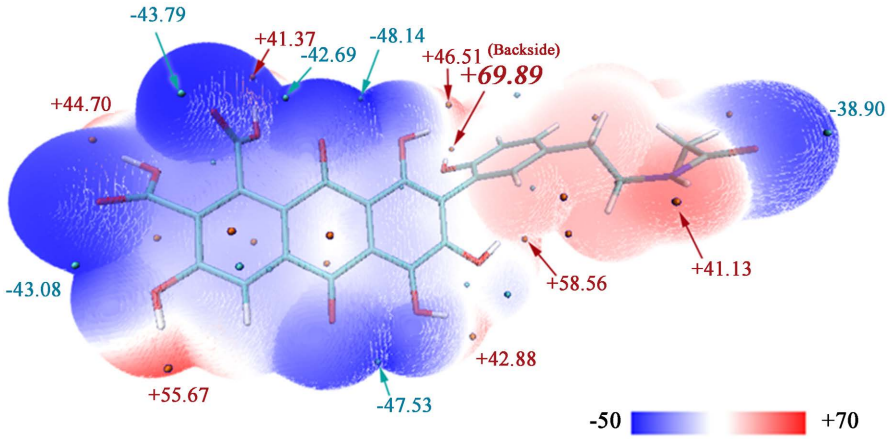

(A)

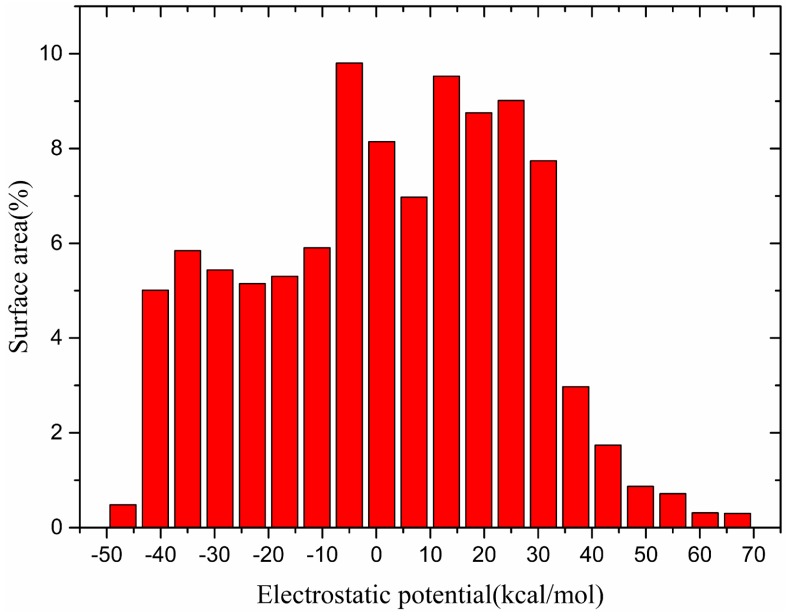

(B)

Figure 8. ESP mapped molecular vdW surface of AA1 and area percent in each ESP range. Significant surface local minima and maxima of ESP are represented as orange and cyan spheres, and labelled by dark blue and brown-red texts, respectively. The transparent ones correspond to the extrema at backside of graph. The unit is in kcal/mol. Only the global minima and maxima on the surface are labelled by italic font.

(−0.610), O28 (−0.682), O30 (−0.616), O42 (−0.624), respectively. Atomic charge distribution of Laccaic acid A will play important role on hydrogen bond interaction or electrostatic attraction toward glycine.

3.3.2. Weak Interaction between Laccaic Acid A and Glycine

The simulation of hydrogen bonds in supramolecular structure elucidates lac red dyes silk fiber by combining the amino acid with two to five hydrogen bonds. **Figures 9(A)-(H)** shows 8 stable compounds without imaginary frequency obtained by structure optimization and frequency calculation of complex space configuration of Laccaic acid A and glycine at B3LYP/6-31G(d) level. The

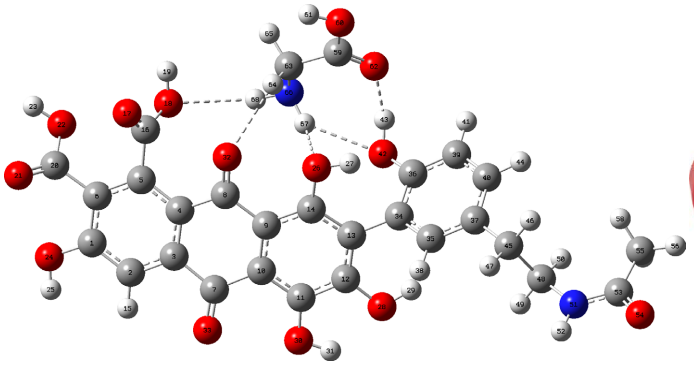

(A)

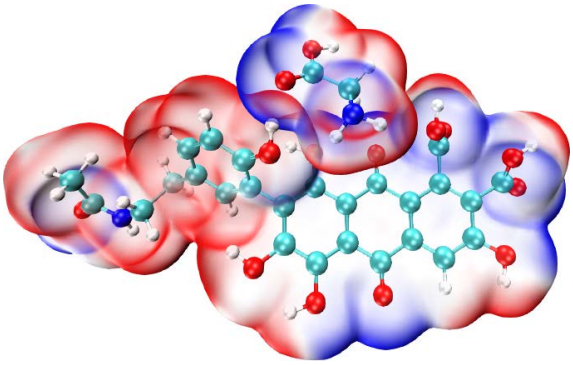

(a)

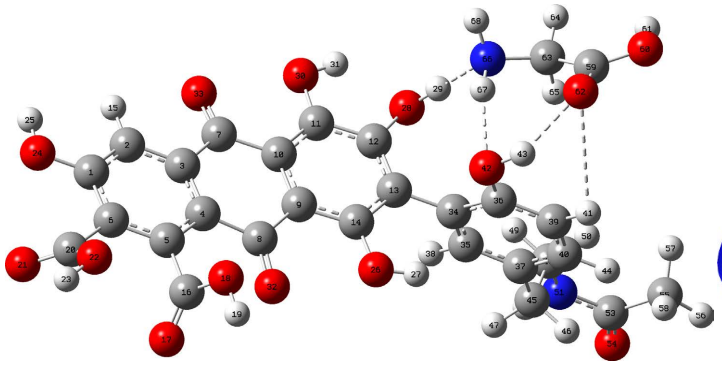

(B)

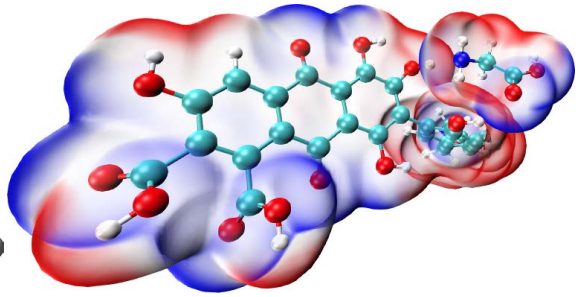

(b)

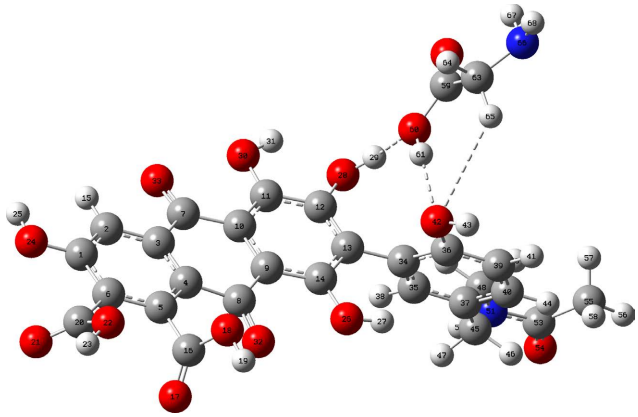

(C)

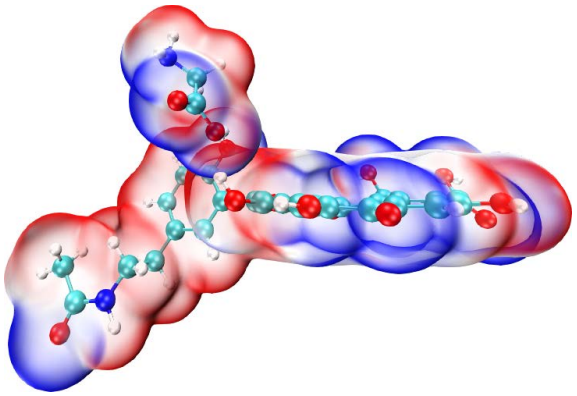

(c)

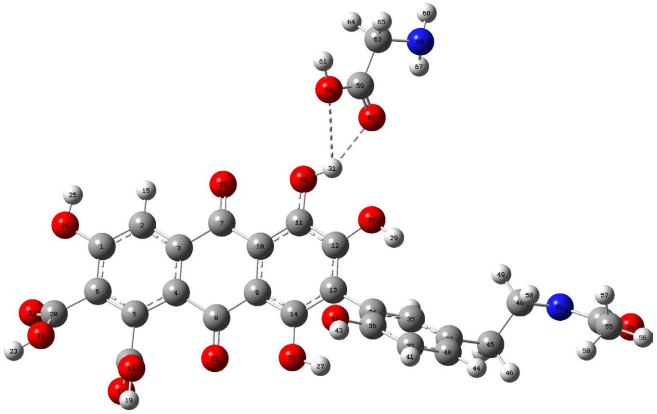

(D)

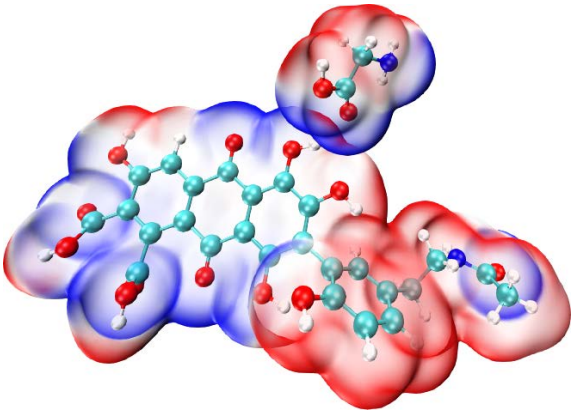

(d)

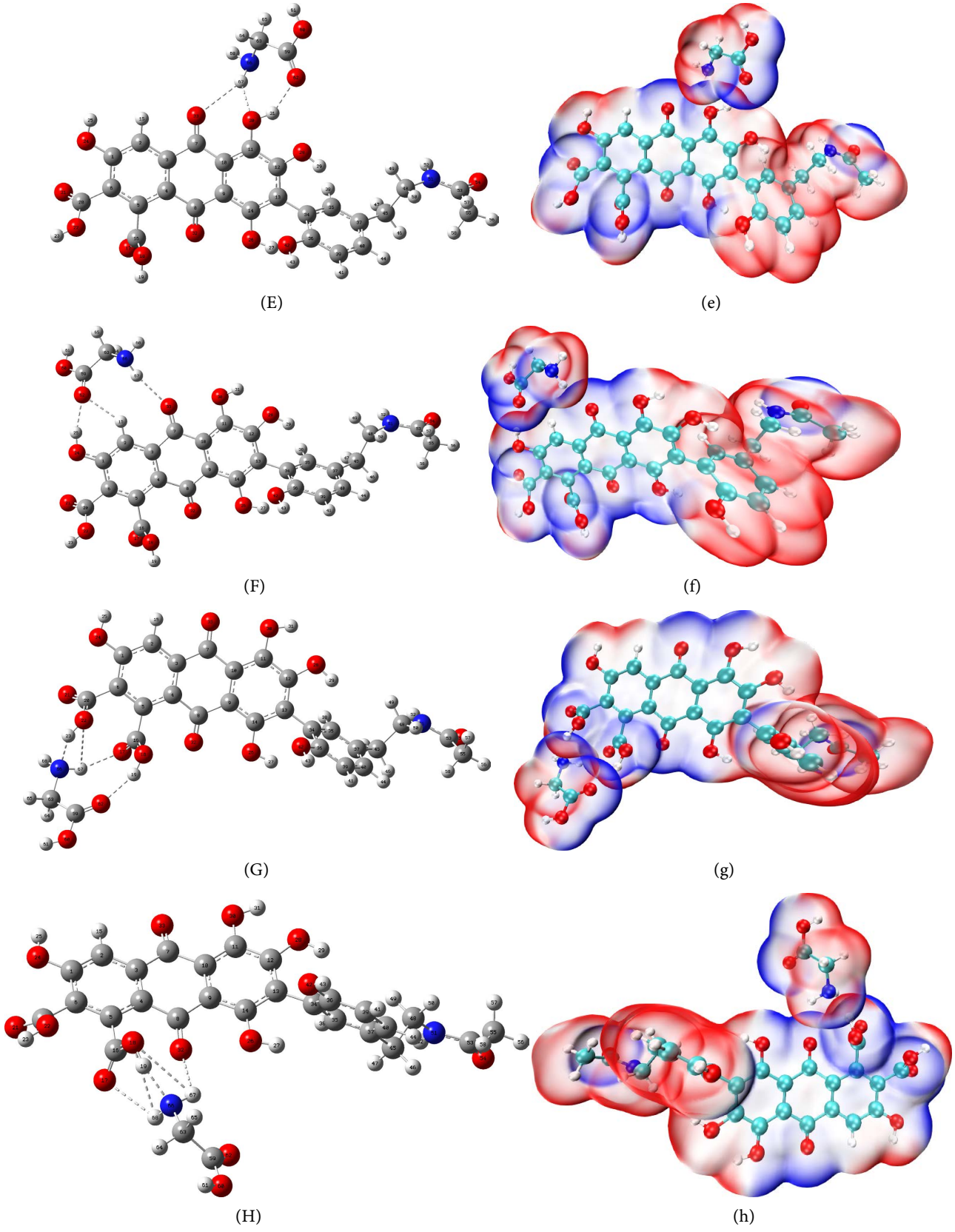

Figure 9. The complexes of lac red and glycine and superposition of ESP mapped vdW surfaces of the glycine and Laccaic acid A monomer in the complex structure.

superposition of the ESP colored vdW surface maps of glycine monomer and Laccaic acid A monomer in the complexes A~H can be seen in Figures 9(a)-(h). Typical hydrogen bonds and bond length of the complexes were summarized in Table 2.

As shown in Figure 9 and Table 2, four type hydrogen bonds (N-H…O, O-H…O, C-H…O, O-H…N) were found in in these compounds. Oxygen atoms in hydroxyl group or carboxyl group of Laccaic acid A formed hydrogen bonds with glycine in three ways: 1:1, 1:2, and 2:1. 1:1 type, an oxygen atom in hydroxyl group or carboxyl group forms hydrogen bond with a hydrogen atom in glycine;

Table 2. Typical hydrogen bonds and bond lengths of the complexes.

Complex	Hydrogen bonds	Average	Bond length
Laccaic acid A			O42-H43 (0.970) O24-H25 (0.971) O28-H29 (0.973) 2C-H15 (1.087) C39-H41 (1.088) O22-H23 (0.976) O30-H31 (0.974) O18-H19 (0.976)
A	N66-H67…O26 (2.649) O42-H43…O62 (1.794) N66-H67…O42 (2.408) C63-H64…O32 (2.469) N66-H68…O18 (2.640)	2.392	O42-H43 (0.987)
B	O28-H29…N66 (1.766) O42-H43…O62 (2.004) N66-H67…O42 (2.018) C39-H41...O52 (2.954)	2.186	O28-H29 (1.005) C39-H41 (1.087) O42-H43 (0.978)
C	O28-H29…O60 (1.889) C63-H65…O42 (2.979) O60-H61…O42 (1.861)	2.243	O28-H29 (0.981)
D	O30-H31…O60 (2.896) O30-H31…O62 (1.945)	2.421	O30-H31 (0.982)
E	N66-H67…O33 (2.492) O30-H31…O62 (1.888) N66-H67…O30 (2.105)	2.162	O30-H31 (0.984)
F	O24-H25…O62 (1.868) N66-H67…O33 (2.179) 2C-H15…O62 (2.275)	2.107	O24-H25 (0.982) 2C-H15 (1.081)
G	O22-H23…N66 (1.827) N66-H67…O17 (2.636) N66-H67…022 (2.756) O18-H19…O62 (1.964)	2.296	O22-H23 (1.003) O18-H19 (0.982)
H	N66-H68…O17 (2.50) N66-H67…O32 (2.479) N66-H68…O18 (2.915) O18-H19…N66 (1.771) N66-H67…O18 (2.942)	2.521	O18-H19 (1.008)

1:2 type, an oxygen atom in hydroxyl group or carboxyl group forms hydrogen bond with two hydrogen atoms in glycine; 2:1, two oxygen atoms in hydroxyl group or carboxyl group form hydrogen bond with a hydrogen atom in glycine. Oxygen atom in quinone group of Laccaic acid A formed hydrogen bonds with glycine in one way: 1:1, such as N66-H67…O33 (2.492Å).

The bond lengths of O42-H43, O24-H25, O28-H29, O22-H23, O30-H31, O18-H19 increased after the formation of complex between l Laccaic acid A and glycine because of the electron withdrawing effect of oxygen atoms and hydrogen atom in glycine, for example, O42-H43 bond length increased from 0.970Å to 0.987Å, whereas the bond lengths of 2C-H15 and C39-H41 decreased.

Binding energy (D_0) means the difference between total energy of Laccaic acid A-glycine complexes and corresponding single molecules (Laccaic acid A and glycine). The total energy of single molecule (Laccaic acid A and glycine) and different complexes was originated from Gaussian simulation according to the following Equation (6).

$$D_0 = -\Delta E = E_L + E_G - E_C \tag{6}$$

where E_L, E_G, E_C show the total energy of corresponding single molecules (Laccaic acid A and glycine) or different complexes, respectively. Total energy (E), binding energy (D_0), and dipole moment were summarized in Table 3.

As shown in Table 3, the binding energy of 8 complexes range from 25.455 - 71.835 kJ/mol and the complexes containing four or five hydrogen bonds are generally more stable than those with two or three hydrogen bonds because the binding energy of the former is higher than the latter. It is worthy noticing that A and H binding energy which have five hydrogen bonds are lower than B binding energy in that the shorter average bond length of B. These phenomena demonstrate hydrogen bond possesses additivity and the stability of complex of lac red and glycine is closely associated with the number and length of hydrogen bonds.

From Figures 9(a)-(h), the inter-penetration between the vdW surfaces of the

Table 3. Binding energy and dipole moment for the complexes on B3LYP/6-31 + G* level.

Complex	Total energy (kJ/mol)	Binding energy (kJ/mol)	Dipole moment (Debye)
A	−5,891,865.93	68.621	3.8041
B	−5,891,869.14	71.835	14.4856
C	−5,891,838.60	41.294	10.8460
D	−5,891,822.76	25.455	12.5432
E	−5,891,838.71	41.406	7.8567
F	−5,891,849.38	52.076	10.5831
G	−5,891,865.24	67.931	7.4061
H	−5,891,859.23	61.925	10.7805

glycine and Laccaic acid A monomer due to formation of hydrogen bonds can be clearly seen. In addition, the mapped colors show that the complexes were formed in ESP positive-negative complementary way, revealing the electrostatic nature of the hydrogen bonds. It is well known that molecules always tend to approach each other in a complementary manner of ESP to maximize electrostatic interaction energy. Therefore, we can also intuitively the structural stability sequence of glycine-Laccaic acid A complexes by simply observing the way and extent of superposition of ESP mapped vdW surfaces.

Dipole moment elucidates the polarity of the complex. The higher dipole moment of the complex clarified a higher polarity of the complex. It was apparent that B which has the highest dipole moment possesses good water solubility.

To sum up, the complex space configuration of Laccaic acid A and glycine was mainly as shown in B when lac red dyed on silk.

3.3.3. Vision Study of Weak Interaction of the Complex B

The noncovalent interaction (NCI) method, which is also known as reduced density gradient (RDG) method, is a popular method in graphically displaying occurrence region and nature of inter-molecular non-covalent interactions. In order to provide a clear insight into the inter-molecular interactions between the Laccaic acid A and glycine monomer of the complex B, we utilized this analysis method see Figure 10. In Figure 10, the regions enclosed by the RDG isosurfaces are where weak interactions present; the mapped color indicates the type of interaction (see the color bar). From this figure, we can very clearly view the H-bonds between the polar groups in Laccia acid A and glycine (blue isosurfaces) as well as the strong steric effect in the aromatic rings (red or orange isosurfaces). According to the color of isosurfaces, it can be seen that 1-hydroxy hydrogen group in Laccaic acid A formed strong H-bonds with and amino group

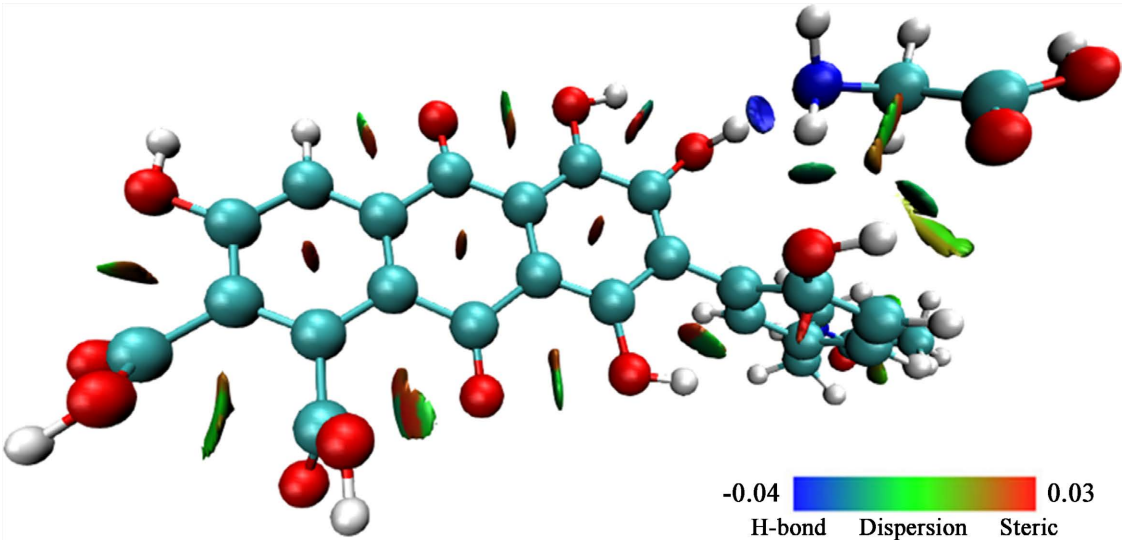

Figure 10. RDG map of the complex B. Reduced density gradient isosurface map of the complex B, isovalue is set to 0.5. The value of Sign(λ^2)ρ in surfaces is represented by filling color according to the color bar in upper left corner.

in glycine (blue isosurfaces). The hydroxyl group on the side chain of Laccaic acid A formed two H-bonds with the amino and hydroxyl groups in glycine, the color in the corresponding RDG isosurfaces is blue-green, manifesting that these two hydrogen bonds are weaker than the first one. It is worth noting that the RDG maps also reveal very weak C39-H41...O62 type of H-bond (green isosurfaces), the strength of H-bond is no different than van der Waals.

4. Conclusions

In this study, different temperatures for the optimization of the dyeing parameters were studied. The optimized dyeing condition of lac red on silk was as follows: 6% o.w.f. of lac dye, a material to liquor ratio of 1:60, pH 3.6, dyeing temperature 60˚C, and 60 min. The optimized dyeing condition of lac red on wool was as follows: 6% o.w.f. of lac dye, a material to liquor ratio of 1:60, pH 3.6, dyeing temperature 90˚C, and 60 min.

The thermodynamics study revealed Nernst isotherm and the Freundlich model fitted well with the adsorption equilibrium data. The mechanism that lac red dyed wool and silk fiber mainly by hydrogen bonding was similar to disperse dyes. The standard affinity ($-\Delta\mu_0$), dyeing enthalpy (ΔH) and dyeing entropy (ΔS) for dye adsorption were also determined, and the negative values of $\Delta\mu$ and ΔH obtained indicated that the lac dye adsorption process is both spontaneous and exothermic.

Density functional theory (DFT) calculations and wavefunction analysis were to gain a comprehensive and deep insight into the intermolecular interaction between Laccaic acid A and glycine. Charge distribution on the vdW surface reveals that the most positive and the most negative ESP regions are present around hydrogen and oxygen atom of carboxyl group, so it is likely that there is a significant electrostatic interaction between Laccaic acid A and glycine at these positions. The ESP colored penetration map of the vdW surface of monomers reveals the electrostatic nature of the hydrogen bonds. The results showed that the natural dyestuff of lac red dyes silk fiber by hydrogen-bond interactions and van der Waals force, which is coincident with the results of dyeing thermodynamics research.

The investigation proved the interaction of lac red on silk fabric mainly depended on weak hydrogen bonds and van der Waals force, which were accountable for low color fastness and poor stability. And hydrogen bond possesses additivity and the stability of the complex of lac red and glycine is closely associated with the number and length of hydrogen bonds.

Acknowledgements

This work was supported by the National Natural Science Foundation of China (No. 51003047). The authors also gratefully appreciated the financial support from the Students Innovation and Entrepreneurship Training Program of Jiangsu Province (2020DC0780, 2021DC0867).

Conflicts of Interest

The authors declare no conflicts of interest regarding the publication of this paper.

References

[1] Gong, H., Zhou, H., Forrest, R.H., Li, S., Wang, J., Dyer, J.M. and Hickford, J.G. (2016) Wool Keratin-Associated Protein Genes in Sheep—A Review. *Genes* (*Basel*), **7**, 24-40. https://doi.org/10.3390/genes7060024

[2] Sarker, P., Hosne Asif, A., Rahman, M., Islam, M. and Rahman, K. (2020) Green Dyeing of Silk Fabric with Turmeric Powder Using Tamarind Seed Coat as Mordant. *Journal of Materials Science and Chemical Engineering*, **8**, 65-80. https://doi.org/10.4236/msce.2020.82007

[3] Vankar, P.S., Shanker, R. and Verma, A. (2007) Enzymatic Natural Dyeing of Cotton and Silk Fabrics without Metal Mordants. *Journal of Cleaner Production*, **15**, 1441-1450. https://doi.org/10.1016/j.jclepro.2006.05.004

[4] Chairat, M., Rattanaphani, S., Bremner, J.B. and Rattanaphani, V. (2005) An Adsorption and Kinetic Study of Lac Dyeing on Silk. *Dyes and Pigments*, **64**, 231-241. https://doi.org/10.1016/j.dyepig.2004.06.009

[5] Burwood, R., Read, G., Schofield, K. and Wright, D.E. (1967) The Pigments of Stick Lac. Part II: The Structure of Laccaic Acid A1. *Journal of the Chemical Society C*, **9**, 842-851. https://doi.org/10.1039/j39670000842

[6] Pandhare, E.D., Rao, A.V.R., Shaikh, I.N. and Venkataraman, K. (1967) The Constitution of Laccaic Acid B. *Wtrahedron Letters*, **26**, 2437-2440. https://doi.org/10.1016/S0040-4039(00)90827-X

[7] Santos, R., Hallett, J., Oliveira, M.C., Sousa, M.M., Sarraguça, J., Simmonds, M.S.J. and Nesbitt, M. (2015) HPLC-DAD-MS Analysis of Colorant and Resinous Components of Lac-Dye: A Comparison between Kerria and Paratachardina Genera. *Dyes and Pigments*, **118**, 129-136. https://doi.org/10.1016/j.dyepig.2015.02.024

[8] Oka, H., Ito, Y., Yamada, S., Kagami, T., Hayakawa, J., Harada, K. and Ito, Y. (1998) Separation of Lac Dye Components by High-Speed Counter-Current Chromatography. *Journal of Chromatography A*, **813**, 71-77. https://doi.org/10.1016/S0021-9673(98)00311-2

[9] Yamada, S., Noda, N., Mikami, E., Hayakawa, J. and Yamada, M. (1989) Analysis of Natural Coloring Matters in Food. III. Application of Methylation with Diazomethane for the Detection of Lac Color. *Journal—Association of Official Analytical Chemists*, **72**, 48-51. https://doi.org/10.1093/jaoac/72.1.48

[10] Wu, C.H. (2007) Adsorption of Reactive Dye onto Carbon Nanotubes: Equilibrium, Kinetics and Thermodynamics. *Journal of Hazardous Materials*, **144**, 93-100. https://doi.org/10.1016/j.jhazmat.2006.09.083

[11] Asif Tahir, M., Bhatti, H.N. and Iqbal, M. (2016) Solar Red and Brittle Blue Direct Dyes Adsorption onto *Eucalyptus angophoroides* Bark: Equilibrium, Kinetics and Thermodynamic Studies. *Journal of Environmental Chemical Engineering*, **4**, 2431-2439. https://doi.org/10.1016/j.jece.2016.04.020

[12] Li, M., Song, K., Xie, K. and Hou, A. (2014) Crystal Morphology, Dispersing Stability and Dyeing Property of the Disperse Dye Based on Benzisothiazole. *Pigment & Resin Technology*, **43**, 365-370. https://doi.org/10.1108/PRT-10-2013-0099

[13] Frisch, M.J., Trucks, G.W., Schlegel, H.B., Scuseria, G.E., Robb, M.A., Cheeseman, J.R., Fox, D.J., *et al.* (2016) Gaussian 16. Revision B.01 Edition, Gaussian Inc., Wallingford.

[14] Yang, Y., Weaver, M.N. and Merz, K.M. (2009) Assessment of the "6-31+G** + LANL2DZ" Mixed Basis Set Coupled with Density Functional Theory Methods and the Effective Core Potential: Prediction of Heats of Formation and Ionization Potentials for First-Row-Transition-Metal Complexes. *The Journal of Physical Chemistry A*, **113**, 9843-9851. https://doi.org/10.1021/jp807643p

[15] Chen, C. and Liu, W. (2017) Research of Dyeing Thermodynamics and Supramolecular Structure of Luteolin on Wool Fabric. *World Journal of Enguneering and Technolgy*, **5**, 20-29.

[16] Qin, M., Zhong, F., Sun, Y., Tan, X., Hu, K., Zhang, H., Zhuang, L., *et al.* (2020) Experimental and DFT Studies on Surface Properties of Sulfonate-Based Surface Active Ionic Liquids. *Journal of Molecular Structure*, **1215**, Article ID: 128258. https://doi.org/10.1016/j.molstruc.2020.128258

[17] Lu, T. and Chen, F. (2012a) Multiwfn: A Multifunctional Wavefunction Analyzer. *Journal of Computational Chemistry*, **33**, 580-592. https://doi.org/10.1002/jcc.22885

[18] Humphrey, W., Dalke, A. and Schulten, K. (1996) VMD: Visual Molecular Dynamics. *Journal of Molecular Graphics*, **14**, 33-38. https://doi.org/10.1016/0263-7855(96)00018-5

[19] Bader, R.F.W., Carroll, M.T., Cheeseman, J.R. and Chang, C. (1987) Properties of Atoms in Molecules: Atomic Volumes. *Journal of the American Chemical Society*, **109**, 7968-7979. https://doi.org/10.1021/ja00260a006

[20] Knyazkov, D.A., Slavinskaya, N.A., Dmitriev, A.M., Shmakov, A.G., Korobeinichev, O.P. and Riedel, U. (2016) Structure of an n-Heptane/Toluene Flame: Molecular Beam Mass Spectrometry and Computer Simulation Investigations. *Combustion, Explosion, and Shock Waves*, **52**, 142-154. https://doi.org/10.1134/S0010508216020039

[21] Chairat, M. (2009) Thermodynamics Study of Lac Dyeing of Silk Yarn Coated with Chitosan. *Journal of Science & Technology*, **6**, 93-107.

[22] Chiou, M.S. and Li, H.Y. (2002) Equilibrium and Kinetic Modeling of Adsorption of Reactive Dye on Cross-Linked Chitosan Beads. *Journal of Hazardous Materials*, **B93**, 233-248. https://doi.org/10.1016/S0304-3894(02)00030-4

[23] Qian, H.F. and Song, X.Y. (2007) The Structure of Azo Disperse Dyes and Its Distribution on Polyurethane Fiber Blend with Polyester, or Polyamide Fiber. *Dyes and Pigments*, **74**, 672-676. https://doi.org/10.1016/j.dyepig.2006.04.011

[24] Khan, M.I., Min, T.K., Azizli, K., Sufian, S., Ullah, H. and Man, Z. (2015) Effective Removal of Methylene Blue from Water Using Phosphoric Acid Based Geopolymers: Synthesis, Characterizations and Adsorption Studies. *RSC Advances*, **5**, 61410-61420. https://doi.org/10.1039/C5RA08255B

[25] Ncibi, M.C., Mahjoub, B. and Seffen, M. (2007) Kinetic and Equilibrium Studies of Methylene Blue Biosorption by *Posidonia oceanica* (L.) Fibres. *Journal of Hazardous Materials*, **139**, 280-285. https://doi.org/10.1016/j.jhazmat.2006.06.029

[26] Chimprasit, A., Bremner, J.B., Danworaphong, S., Sajomsang, W., Gonil, P. and Chairat, M. (2019) A Kinetic and Thermodynamic Study of Lac Dye Adsorption on Silk Yarn Coated with Microcrystalline Chitosan. *Coloration Technology*, **135**, 224-233. https://doi.org/10.1111/cote.12396

[27] Lu, T. and Chen, F. (2012b) Quantitative Analysis of Molecular Surface Based on Improved Marching Tetrahedra Algorithm. *Journal of Molecular Graphics and Modelling*, **38**, 314-323. https://doi.org/10.1016/j.jmgm.2012.07.004

[28] Manzetti, S. and Lu, T. (2013) The Geometry and Electronic Structure of Aristolochic Acid: Possible Implications for a Frozen Resonance. *Journal of Physical Or-*

ganic Chemistry, **26**, 473-483. https://doi.org/10.1002/poc.3111

[29] Lu, T. and Chen, F. (2013) Revealing the Nature of Intermolecular Interaction and Configurational Preference of the Nonpolar Molecular Dimers $(H_2)_2$, $(N_2)_2$, and $(H_2)(N_2)$. *Journal of Molecular Modeling,* **19**, 5387-5395. https://doi.org/10.1007/s00894-013-2034-2

[30] Lu, T. and Manzetti, S. (2014) Wavefunction and Reactivity Study of Benzo[a]pyrene Diol Epoxide and Its Enantiomeric Forms. *Structural Chemistry,* **25**, 1521-1533. https://doi.org/10.1007/s11224-014-0430-6

[31] Johnson, E.R., Keinan, S., Mori-Sanchez, P., Contreras-Garcia, J., Cohen, A.J. and Yang, W. (2010) Revealing Noncovalent Interactions. *Journal of the American Chemical Society,* **132**, 6498-6506. https://doi.org/10.1021/ja100936w

[32] Chairat, M., Rattanaphani, V., Bremner, J.B., Rattanaphani, S. and Perkins, D.F. (2004) An Absorption Spectroscopic Investigation of the Interaction of Lac Dyes with Metal Ions. *Dyes and Pigments*, **63**, 141-150. https://doi.org/10.1016/j.dyepig.2004.02.006